

# Health Management and Prognostics for Electric Aircraft Powertrain

Chetan Kulkarni\*

*SGT. Inc, NASA Ames Research Center, Moffett Field, CA 94035, USA*

Matteo Corbetta†

*SGT. Inc, NASA Ames Research Center, Moffett Field, CA 94035, USA*

With significant improvement in battery technology, electrically-powered autonomous vehicles are being increasingly considered to develop vehicles to transport packages, and critical material such as medical applications, for inter as well as intra-city operations. Any air borne vehicle needs incorporating safety as key parameter of measure, and inclusion of autonomy raises the critical need for safety under autonomous operations.

Management of faults and component degradation is key as complexity in autonomous operations grow over the period of time. Therefore, in addition to basic operational requirements, an autonomous electric vehicle should be able to make accurate estimates of its current system health and take the correct decisions to complete its mission successfully. Real-time safety and state-awareness tools are therefore essential for the vehicle to be able to reach its destination in a safe and successful manner.

The need for safety assurance and health management capabilities is particularly relevant for aircraft electric propulsion systems, which are relatively new and with limited historical to learn. They are critical systems requiring high power density along with reliability, resilience, efficient management of weight, and operational costs. A model-based fault diagnosis and prognostics approach of complex critical systems can successfully accomplish the safety and state awareness goal for such electric propulsion systems, enabling autonomous decision making capability for safe and efficient operation. To identify critical components in the system a Qualitative Bayesian approach using FMECA is implemented. This requires the assessment of some quantities representing the state of the electric unmanned aerial systems (e-UAS), as well as look-ahead forecasts of such states during the entire flight, presented in form of safety metrics (SM).

In-service data and performance data gathered from degraded components supports diagnostic and prognostic methods for these systems, but this data can be difficult to obtain as weight and packaging restrictions reduce redundancy and instrumentation on-board the vehicle. Therefore, an model-based framework should be capable or operating with limited data.

In addition to data scarcity, the variability of such complex critical systems requires the model-based framework to reason in the presence of uncertainty, such as sensor noise, and modeling imperfections. Quantification of errors and uncertainties in the measured states and quantities is therefore a fundamental step for a precise estimation of such SMs; un-modeled uncertainty may result in erroneous state assessment and unreliable predictions of future states of e-UAVs. Typical, centralized model-based schemes suffer from inherent disadvantages such as computational complexity, single point of failure, and scalability issues, and therefore may fail in such a complex scenario.

This paper presents a methodology for developing a system level diagnostics and prognostics approach using a Qualitative Bayesian FMECA approach along with a formal uncertainty management framework for an e-UAS. In this work we demonstrate the efficacy of the framework to predict effects of sub-system level degradation on vehicle operation incorporating uncertainty management to predict future behavior under different operating conditions.

---

\*Intelligent Systems Division, Discovery and Systems Health Area, MS 269-3, Senior AIAA Member

†Intelligent Systems Division, Discovery and Systems Health Area, MS 269-3, AIAA Member

## I. Introduction

With accelerated improvement in battery technology, progress in developing a practical vehicle to deliver packages as well as critical items such as medical services has increased proportionally. The trend is inclined more towards operating in a fully- or semi-autonomous mode. This inclusion of autonomy raises the critical need for incorporating safety under autonomous operations into system operations. An autonomous electric vehicle should be able to make accurate estimates of its current health state and take the right decisions to deliver the critical package on time to complete its mission successfully. This requires assessing the health state of its own critical systems, which in this case is the electrical propulsion system, for it to be able to reach its destination in a safe and successful manner.

Electric propulsion systems for aircraft require reliability, resilience, and high power density. These systems must also manage weight, complexity, and operational costs. As more aircraft transition to electric propulsion systems, the management of faults and component degradation becomes increasingly important. Implementation of a diagnosis and prognosis framework of complex critical systems enables their safe and efficient operation which monitors and updates health state of these critical systems. This is done by developing a combined Failure mode, effects and criticality analysis (FMECA) based framework wherein sub-systems and components are selected for health monitoring based on their criticality and probability of failure.

Typically, model-based schemes are centralized approaches that suffer from inherent disadvantages such as computational complexity, single point of failure, and scalability issues. Distributing the task within the overall system framework addresses these issues. To this end, this paper presents development of the process flow to implement a health monitoring framework for an electric unmanned aerial systems (e-UAS). The presented framework is limited to an electrical power-train of the e-UAS.

In order to perform system-level prognostics on electric power-train systems, the first step is to identify subsystems that have higher probability failure using a combined FMECA and Qualitative Bayesian approach. A distributed diagnosis approach is implemented to detect and diagnose the power-train subsystem<sup>1</sup> that has failed which then instantiates the prognoser for estimating remaining useful life (RUL) of the faulty system or component. In addition, quantification and management of uncertainty is equally important since it drives the performance of both diagnostic and prognostic systems. Embedding uncertainty quantification techniques is particularly relevant for the proposed frameworks, which leverages several models and algorithms, each one of those with different levels of model abstractions, simplifying hypotheses, and accuracy. Therefore, this paper also introduces a preliminary assessment of the sources of uncertainty affecting the framework, and a discussion on uncertainty representation techniques for the key elements of the system; battery, electronic speed controller (ESC), and motors being used in an e-UAS.

The rest of the paper is organized as follows. Section II outlines motivation and background for this work. Section III discuss FMECA framework developed for the power-train. Section IV discusses the use of FMECA with quantitative and qualitative Bayesian analysis to enhance fault isolation and diagnosis. In Section V details of electric modeling power-train subsystems of a multi-rotor vehicle is discussed. Section VI and VII describes the distributed diagnosis and prognostics approaches. Section VIII discuss uncertainty quantification and implementation for electric power-trains. Conclusions and future work are discussed in Section IX.

## II. Motivation and Background

The fundamental components of a power-train in an electrically powered rotor-craft include key electrical components such as batteries, motors, and power electronics such as electronic speed controllers (ESC) and conditioning electronic systems (CES). The motivation for this work evolved from flight operations with the all-electric Edge 540T UAV<sup>2</sup> fixed wing UAV, where during test flights abnormally high current draw was observed from one of the batteries. Investigation of the flight data and troubleshooting confirmed that one of the ESC's on the UAV had aged and degraded since the vehicle was commissioned, leading to degradation in UAS operational performance. This lead to studies for investigating other systems in an electrical power-train and formulate methodology to implement a health monitoring framework.

Earlier research work presented in<sup>3,4</sup> focused on individual systems and components to implement prognostics methodologies. In the later approaches effects of component-level degradation on the system as a whole<sup>5,6</sup> were studied to implement the prognostics framework. The development of new models and in-

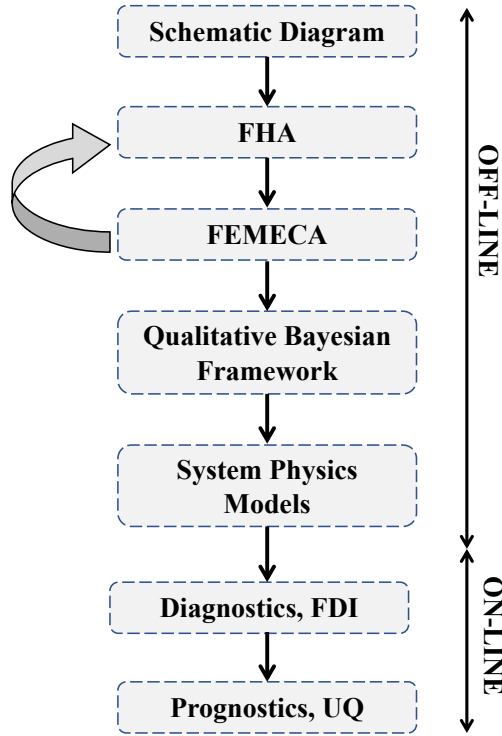


**Figure 1. Process Flow Chart of the implemented approach to UAV Health Management**

tegration with previous models enables to study and identify cascaded effects of degradation on connected power-train systems during operation. In Hogge et. al,<sup>2</sup> implementation of prognostic framework to batteries in fixed wing e-UAS was studied.

As briefly discussed in I in this work a process flow as shown is Fig. 1 to implement integrated FMECA and Qualitative Bayesian approach incorporating distributed fault diagnosis and prognosis to Health monitoring is presented. In addition uncertainty quantification techniques are embedded into the framework to take into account of model abstractions, simplifying hypotheses, and estimation accuracy.

### III. e-UAS Powertrain FMECA

Functional Hazard analysis (FHA) of a given system is the first step in a process to assess any associated risk of failure in the system. The output results obtained from the hazard analysis processes assess the different type of hazards along with their probability of failures. These can be qualitative i.e high, low as well as quantitative i.e. 1 or 0. In this work and qualitative approach is being implemented. The probability of failure in a system can be linked with multiple events or cascading effects down the system finally leading to an accident. A combined sequence of such activities is called a scenario. Depending upon the types of system faults a single system can have different potential accident scenarios which can range from high - low probability of occurrence.

FMECA is a bottom-up, inferred analytical method which includes criticality analysis, used to map the probability of failure modes with the severity of their consequences. The resultant map shows failure modes with in relationship with probability and severity of consequences.

Fig. 2 shows a schematic line diagram for a quad-rotor e-UAS propulsion system. The system as show consists of four motors ( $M_{1-4}$ ), which are controlled by four ESC controllers ( $ESC_{1-4}$ ). All the four motor controllers are governed by power controller system (PCS) and battery pack consisting of several smaller packs. Though in a real operational system each of the battery pack will be monitored in this work B1-B4 are considered as a single battery pack.

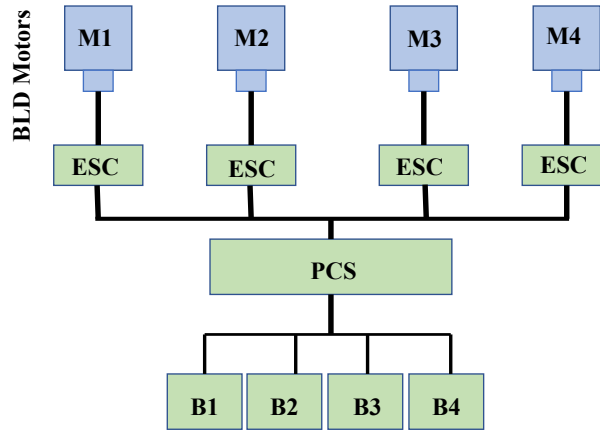


**Figure 2. Schematic of an Quad-rotor Electric UAS Propulsion System**

#### IV. Qualitative Bayesian Theorem Approach

Bayesian theorem concepts can be implemented using quantitative as well as qualitative methods.<sup>7,8</sup> It is very important to know prior probabilities based on operational knowledge and feedback from SME's to implement the approach. Details of known failure probabilities for an e-UAS system are as shown in Table. 1. This can be expressed categorically as low (less likely than 10%), medium (between 10% and 66%), high (between 67% and 90%) or extreme (more likely than 90%). For example, if battery SOC has a high probability of failure, then in this case, if an fault observed due to voltage decrease it can be detected/isolated as an SOC fault as mapped in the FMECA table.

If the probability is in one of the intermediate categories, then further analysis is required which is detected by the fault diagnosis framework. Further once the fault is detected and isolated the next step is to make a prognostics estimation for remaining useful time (RUL) till the predetermined lower bound threshold of SOC of a battery pack is reached.

**Table 1. FMECA for e-UAS Power-train System**

Component	Faults	Root Cause	Effect on UAV	Effect on Airspace	Severity	Probability of Occurrence	Safety Critical
Battert Pack	SOC	Operational Conditions	Directly affects operation of the power train system	In case the SOC goes below set low threshold and UAV is not able to do a safe landing may violate safety with crash landing/ may interfere in path of other UAV	High	High	High
Battery Pack	SOH	Operational conditions, loading profiles	Aging in the batteries may not directly affect other systems	The UAV may not able to do certain maneuvers within required time period	High	High	High
Motor (Single)	Low insulation resistance	Operational conditions, loading profiles	Aging in the batteries may not directly affect other systems	The UAV may not able to do certain maneuvers within required time period	High	High	High
Motor (Single)	Bearing Faults, mass unbalance	Operational conditions, loading profiles	Aging in the batteries may not directly affect other systems	The UAV may not able to do certain maneuvers within required time period	High	High	High
Motor (Single)	Power Consumption	change in winding resistance, bearing faults	High draw currents decrease the battery RUL shortening flight time considerably	In case the SOC goes below set low threshold and UAV is not able to do a safe landing may violate safety with crash landing/ may interfere in path of other UAV	Medium	Medium	Low
Motor (Multiple)	Power Consumption, Low insulation resistance, bearings	change in winding resistance, bearing faults	High draw currents decrease the battery RUL shortening flight time considerably	In case the SOC goes below set low threshold and UAV is not able to do a safe landing may violate safety with crash landing/ may interfere in path of other UAV	High	Low	High
ESC (Single)	Power Consumption	operational stress, High electrical, thermal stress on the components	Change in switching frequency, MOSFET degradation, stuck faults	The UAV may not able to do certain maneuvers within required time period and flight profile	Medium	Low	Low
ESC (Multiple)	Power Consumption	operational stress, High electrical, thermal stress on the components	Change in switching frequency, MOSFET degradation, stuck faults	The UAV may not able to do certain maneuvers within required time period and flight profile	High	Low	High
CES	Filtering Capacitor/MOSFET failures	Operational stress, High electrical, thermal stress on the components	Directly affects operation of the power train system	The UAV may not able to do certain maneuvers within required time period and flight profile	High	Low	High

## V. Electrical Propulsion System Modeling

With reference to Figure. 1 the initial steps for FMECA development and Qualitative Bayesian framework are discussed in the prior sections. In this work an model based Fault Detection and prognostics estimation methodology<sup>9</sup> is being implemented. This is the last OFF-LINE step in the process before the framework being implemented for the ON-LINE process. Modeling methodologies used to represent system dynamics are generally classified as: (i) empirical models; (ii) engineering models; (iii) multi-physics models; and (iv) molecular/atomist models. Once the sub-systems and components are identified and ranked based on the failure probabilities the next is to develop the models for these sub-systems.

In this section individual sub-system models are developed for the Li-ion batteries, ESC, CES and Brushless DC (BLDC) motor system respectively to be used for the ON-LINE process.

The developed system models are then connected to form the entire electrical propulsion system for simulation in MATLAB. MATLAB Simulink 2017 is used for simulating the entire system as well as injecting faults.

### A. Battery System

A battery is a collection of electrochemical cells that convert between chemical and electrical energy. Each cell consists of a positive electrode and a negative electrode with electrolyte. In this paper, we focus on Li-ion cells. The electrolyte enables lithium ions ( $\text{Li}^+$ ) to diffuse between the positive and negative electrodes. The lithium ions insert or deinsert from the active material depending upon the electrode and whether the active process is charging or discharging.<sup>10</sup>

In this work, we use an electrochemistry-based model developed for Li-ion cells in our previous work.<sup>11</sup> Unlike other electrochemistry-based models that rely on complex partial differential equations that are unsuitable for online estimation and prediction algorithms, this model uses only ordinary differential equations, and is fast enough for real-time use. In this section, we briefly summarize this model and describe its key features.

The voltage terms of the battery are expressed as functions of the amount of charge in the electrodes. Each electrode, positive (subscript  $p$ ) and negative (subscript  $n$ ), is split into two volumes, a surface layer (subscript  $s$ ) and a bulk layer (subscript  $b$ ). The differential equations for the battery describe how charge moves through these volumes. The charge ( $q$ ) variables are described using

$$\dot{q}_{s,p} = i_{app} + \dot{q}_{bs,p} \quad (1)$$

$$\dot{q}_{b,p} = -\dot{q}_{bs,p} + i_{app} - i_{app} \quad (2)$$

$$\dot{q}_{b,n} = -\dot{q}_{bs,n} + i_{app} - i_{app} \quad (3)$$

$$\dot{q}_{s,n} = -i_{app} + \dot{q}_{bs,n}, \quad (4)$$

where  $i_{app}$  is the applied electric current. The  $\dot{q}_{bs,i}$  term describes diffusion from the bulk to surface layer for electrode  $i$ , where  $i = n$  or  $i = p$ :

$$\dot{q}_{bs,i} = \frac{1}{D}(c_{b,i} - c_{s,i}), \quad (5)$$

where  $D$  is the diffusion constant. The  $c$  terms are Li-ion concentrations:

$$c_{b,i} = \frac{q_{b,i}}{v_{b,i}} \quad (6)$$

$$c_{s,i} = \frac{q_{s,i}}{v_{s,i}}, \quad (7)$$

Here,  $c_{v,i}$  is the concentration of charge in electrode  $i$ , and  $v_{v,i}$  is the total volume of charge storage capability. We define  $v_i = v_{b,i} + v_{s,i}$ . Note now that the following relations hold:

$$q_p = q_{s,p} + q_{b,p} \quad (8)$$

$$q_n = q_{s,n} + q_{b,n} \quad (9)$$

$$q^{\max} = q_{s,p} + q_{b,p} + q_{s,n} + q_{b,n}. \quad (10)$$

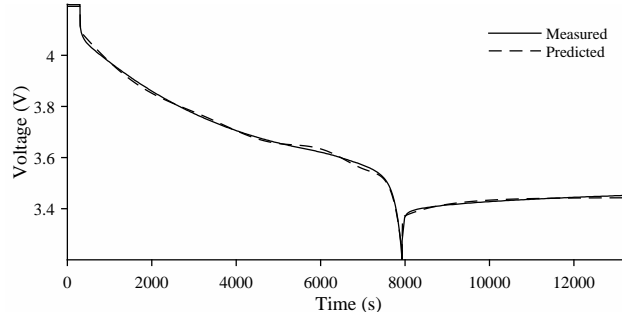


**Figure 3. Battery voltage during 1 A discharge cycle.**

We can also express mole fractions ( $x$ ) based on the  $q$  variables:

$$x_i = \frac{q_i}{q^{\max}}, \quad (11)$$

$$x_{s,i} = \frac{q_{s,i}}{q_{s,i}^{\max}}, \quad (12)$$

$$x_{b,i} = \frac{q_{b,i}}{q_{b,i}^{\max}}, \quad (13)$$

where  $q^{\max} = q_p + q_n$  refers to the total amount of available Li-ions. It follows that  $x_p + x_n = 1$ . For Li-ion batteries, when fully charged,  $x_p = 0.4$  and  $x_n = 0.6$ . When fully discharged,  $x_p = 1$  and  $x_n = 0$ .<sup>12</sup>

The overall battery voltage  $V(t)$  consists of several electrochemical potentials. At the positive current collector is the equilibrium potential  $V_{U,p}$ . This voltage is then reduced by  $V_{s,p}$ , due to the solid-phase ohmic resistance, and  $V_{\eta,p}$ , the surface overpotential. The electrolyte ohmic resistance then causes another drop  $V_e$ . At the negative electrode, there is a drop  $V_{\eta,n}$  due to the surface overpotential, and a drop  $V_{s,n}$  due to the solid-phase resistance. The voltage drops again due to the equilibrium potential at the negative current collector  $V_{U,n}$ .

The state vector, input vector, and output vector of the EOD model are defined follows:

$$\mathbf{x}_{\text{EOD}}(t) = \begin{bmatrix} q_{s,p} & q_{b,p} & q_{b,n} & q_{s,n} & V'_o & V'_{\eta,p} & V'_{\eta,n} \end{bmatrix}^T, \quad (14)$$

$$\mathbf{u}(t) = \begin{bmatrix} i_{app} \end{bmatrix}, \quad (15)$$

$$\mathbf{y}(t) = \begin{bmatrix} V \end{bmatrix}. \quad (16)$$

Detailed equations for each voltage equations and parameter values for a typical Li-ion cell are given in Daigle et al.<sup>11</sup>

An example discharge cycle is shown in Fig. 3. The cell is fully charged at 4.2 V and is discharged at 1 A. At 8000 s, the voltage hits the lower voltage limit, 3.2 V, which defines end-of-discharge (EOD) indicating lower limit of operation. At this point the load is removed and the cell voltage recovers back to the equilibrium potential. Here, we use 3.2 V as the voltage threshold defining EOD. In this case, the capacity is computed as the discharge time (7630 s) times the applied current (1 A), yielding in this case 2.12 Ah.

Note that capacity can only be measured consistently for a discharge cycle at reference conditions, since measured capacity is a nonlinear function of the load and environmental conditions. In this work, reference conditions are defined by a 1 A discharge at room temperature.

## B. Electronic Speed Control System

For the purposes of this research the ESC is modeled as an ideal power inverter employing sinusoidal pulse width modulation (SPWM) and half bridge drivers for each of three phases within a control block. Additionally, power switching devices are also modeled as ideal within the switching function block which represents the commutation functions of the ESC. This enables the study of switching faults, including open-circuit

faults and short-circuit faults, and switching frequency faults such as shoot-through faults. This modeling scheme is representative of general ESC operation for PDC motors which involves battery input, pulse width modulation (PWM) input to control frequency, bridge drivers, and a semiconductor commutation circuit made up of switching transistors. Details of model development are discussed in .<sup>5</sup>

Within the switching function block, F1, F2 and F3 are the PWM signals from the control block and are multiplied by the input voltage V .<sup>5</sup> This amplifies the PWM signal that drives the 3 phase inverter. The output of the function is a 3-phase voltage, Va, Vb, and Vc, that is then connected to a wye motor function block in MATLAB given by Equation 17. F1, F2 and F3 are the outputs from the controlled block while  $v_{ab}$ ,  $v_{bc}$ ,  $v_{ca}$  are the winding voltages between respective phases.

$$\begin{bmatrix} 1 & -1 & 0 \\ 0 & 1 & -1 \\ -1 & 0 & 1 \end{bmatrix} V \begin{bmatrix} F1 \\ F2 \\ F3 \end{bmatrix} = \begin{bmatrix} v_{ab} \\ v_{bc} \\ v_{ca} \end{bmatrix} \quad (17)$$

The developed model is used to both simulate nominal as well as fault injected scenario operation of ESC. The data generated by this model in simulation can be directly compared with empirical data from laboratory testing.

### C. Motor System

The dynamic model of the motor describes a three-phase brushless DC motor, with wye-connected stator windings and a permanent magnet as the rotor. This dynamic model only describes the mechanical device, and assumes that the electronic speed controller provides a given input to the three-phase terminals. Details of the developed model are discussed in .<sup>5</sup>

If the three phase input voltage and back-emf trapezoids are given, then Equations 18, 19, and 20 can be used as the dynamic equations of the brushless DC motor .<sup>5</sup>

$$\frac{d\omega_m}{dt} = \frac{1}{J}(-B\omega_m + (T_e(e, i) - T_l)), \quad (18)$$

where  $J$  is the inertia,  $B$  is the frictional coefficient, and  $T_l$  is the load torque on the rotor. Additionally, the rotor position,  $\theta_m$  is

$$\frac{d\theta_m}{dt} = \frac{p}{2}\omega_m, \quad (19)$$

where  $p$  is the number of poles, and

$$\frac{d}{dt} \begin{bmatrix} i_a \\ i_b \end{bmatrix} = -\frac{R_s}{L_M} \begin{bmatrix} i_a \\ i_b \end{bmatrix} + \frac{1}{L_M} \begin{bmatrix} 2 & 1 \\ 1 & 1 \end{bmatrix} \begin{bmatrix} v_{ab} \\ v_{bc} \end{bmatrix} - \frac{1}{L_M} \begin{bmatrix} 2 & -1 & -1 \\ 1 & 0 & -1 \end{bmatrix} \begin{bmatrix} e_a \\ e_b \\ e_c \end{bmatrix}. \quad (20)$$

## VI. Model Based Diagnostics Approach

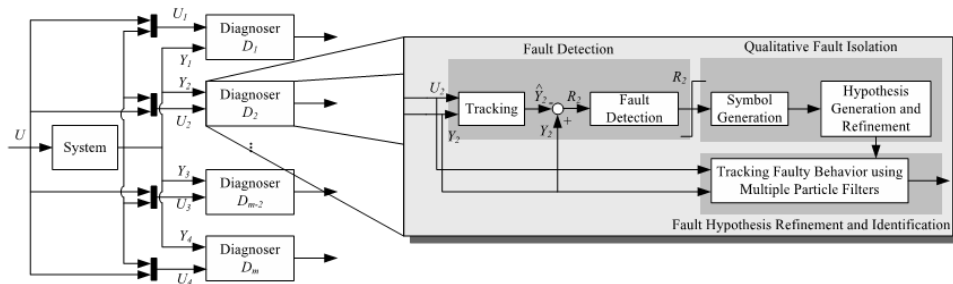


Figure 4. The distributed diagnosis architecture.

Model based diagnosis of complex systems enables their safe and efficient operation. Most model-based diagnosis schemes are centralized approaches that suffer from inherent disadvantages such as computational

complexity, single point of failure, and scalability issues. Distributing the diagnosis task addresses these issues. This work is an application paper that discusses the implementation of our distributed health monitoring approach developed as part of earlier work.<sup>13</sup>

Our distributed diagnosis scheme does not use a centralized coordinator, and each local diagnoser generates globally correct diagnosis results through local analysis, by only communicating a minimal number of measurements with other local diagnosers. The diagnoser design is based on the second algorithm presented in<sup>13</sup> that creates a partition structure and local diagnosers simultaneously. For each local diagnoser, separate particle filter (PF) based inference algorithms for fault detection, isolation, and identification are implemented. The quantitative diagnosis scheme is employed in combination with a qualitative fault isolation scheme to improve diagnosis efficiency. The schematic of our distributed diagnosis approach is shown in Fig. 5. Each local diagnoser performs three primary tasks: (i) fault detection, (ii) qualitative fault isolation (Qual-FI), and (iii) quantitative fault hypothesis refinement and identification (Quant-FHRI).

The fault hypothesis refinement and identification (FHRI) scheme is invoked when either the fault hypotheses set is refined to a pre-defined size,  $k$ , a design parameter, or a pre-specified simulation time-steps have elapsed. For each fault hypothesis that remains when FHRI is initiated, a faulty system model is generated by extending the nominal model used by the local diagnoser to include the fault parameter as a stochastic variable. Again, a PF scheme for each fault model tracks the faulty observed behavior, taking as input the measurements from time  $t_d - \Delta^{max}$ , where  $\Delta^{max} \geq t_d - t_f$  is the maximum delay possible between the time of fault occurrence,  $t_f$ , and the time of fault detection,  $t_d$ . For each PF, a Z-test is used to determine if the deviation of a measurement estimated by the PF from the corresponding actual observation is statistically significant.

As more observations are obtained, ideally the PF using the correct fault model will eventually converge to the observed measurements, while the observations estimated using the incorrect fault models would gradually deviate from the observed measurements. We assume that the particles for the true fault model will converge to the observed measurements within  $s_d$  time steps of its invocation. Since the fault magnitude is included as a stochastic variable in every fault model, the magnitude of the true fault (i.e., the % bias) is considered to be that estimated by the PF for the true fault model.

## VII. Model-based Prognostics Approach

In this section, the end-of-life (EOL) estimation problem is methodically devised using the model-based prognostics framework. The formulation of the problem is based on our earlier work discussed in .<sup>4</sup> Each of the sub-system discussed presents how the developed models can be used for the ON-LINE process.

### A. Problem Formulation

The system model is generally defined as :

$$\mathbf{x}(k+1) = \mathbf{f}(k, \mathbf{x}(k), \boldsymbol{\theta}(k), \mathbf{u}(k), \mathbf{v}(k)), \quad (21)$$

$$\mathbf{y}(k) = \mathbf{h}(k, \mathbf{x}(k), \boldsymbol{\theta}(k), \mathbf{u}(k), \mathbf{n}(k)), \quad (22)$$

where  $k$  is the discrete time variable,  $\mathbf{x}(k) \in \mathbb{R}^{n_x}$  is the state vector,  $\boldsymbol{\theta}(k) \in \mathbb{R}^{n_\theta}$  is the unknown parameter vector,  $\mathbf{u}(k) \in \mathbb{R}^{n_u}$  is the input vector,  $\mathbf{v}(k) \in \mathbb{R}^{n_v}$  is the process noise vector,  $\mathbf{f}$  is the state equation,  $\mathbf{y}(k) \in \mathbb{R}^{n_y}$  is the output vector,  $\mathbf{n}(k) \in \mathbb{R}^{n_n}$  is the measurement noise vector, and  $\mathbf{h}$  is the output equation.<sup>a</sup> The unknown parameter vector  $\boldsymbol{\theta}(k)$  is used to capture explicit model parameters where the values are time-varying stochastically.

The goal of prognostics methodology is to predict the phenomenon event  $E$  that is defined with respect to the states, parameters, and inputs of the system. The event is defined as the earliest instant that event threshold  $T_E : \mathbb{R}^{n_x} \times \mathbb{R}^{n_\theta} \times \mathbb{R}^{n_u} \rightarrow \mathbb{B}$ , where  $\mathbb{B} \triangleq \{0, 1\}$ , goes from the value 0 to 1. That is, the time of the event  $k_E$  at some time of prediction  $k_P$  is defined as

$$k_E(k_P) \triangleq \inf\{k \in \mathbb{N} : k \geq k_P \wedge T_E(\mathbf{x}(k), \boldsymbol{\theta}(k), \mathbf{u}(k)) = 1\}. \quad (23)$$

For example in case of a battery system model there are two prognostics problems, and two corresponding system models, EOD and EOL respectively. These may vary for each sub-system for which the framework

<sup>a</sup>Bold typeface denotes vectors, and  $n_a$  denotes the length of a vector  $\mathbf{a}$ .

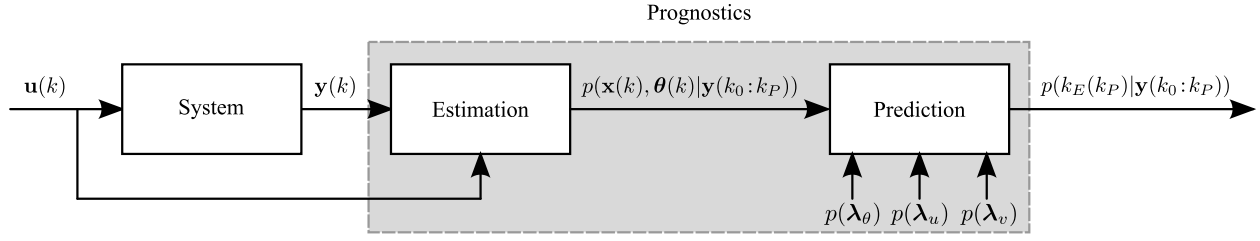


Figure 5. Prognostics Architecture for sub-systems

is applied. For EOD prediction, the event  $E$  represents EOD determined by a voltage threshold; the battery is considered to be at EOD when the voltage goes below a set voltage threshold limit. In this case, an assumption is done that there are no unknown parameters (i.e.,  $\theta = \emptyset$ ). For EOL prediction, the event  $E$  represents EOL and is determined by a set capacity lower threshold for a reference discharge.

## B. Prognostics Architecture

In a model-based prognostics architecture,<sup>14,15</sup> there are two sequential problems, (i) the *estimation* problem, which determines a joint state-parameter estimate  $p(\mathbf{x}(k), \theta(k)|\mathbf{Y}_{k_0}^{k_P})$  based on the history of observations up to time  $k$ , denoted as  $\mathbf{Y}_{k_0}^k$ , and (ii) the *prediction* problem, which determines at prediction time  $k_P$ , using  $p(\mathbf{x}(k), \theta(k)|\mathbf{Y}_{k_0}^{k_P})$ ,  $p(\mathbf{U}_{k_P})$ ,  $p(\mathbf{V}_{k_P})$ , and  $p(\Theta_{k_P})$ , the probability distribution  $p(k_E(k_P)|\mathbf{Y}_{k_0}^{k_P})$ . Here,  $\mathbf{U}_{k_P}$  denotes the future system inputs from  $k_P$  on,  $\mathbf{V}_{k_P}$  denotes the future process noise values from  $k_P$  on, and  $\Theta_{k_P}$  denotes the future unknown parameter values from  $k_P$  on.

In this work, an assumption is made where  $\Theta_{k_P}$  is known exactly,  $\mathbf{V}_{k_P}$  is zero, and  $\mathbf{U}_{k_P}$  is known exactly, in order to focus on validation of the aging models and the performance of the associated predictions. A general framework for dealing with all sources of uncertainty in prognostics is discussed in the next section.

The overall combined EOD/EOL prognostics architecture is shown in Fig. 5. In discrete time  $k$ , the system is provided with inputs  $\mathbf{u}(k)$  (current) and provides measured outputs  $\mathbf{y}(k)$  (voltage). There are two models used for the two different prediction problems: one for EOD (with subscript EOD), and one for EOL (with subscript EOL). The age parameter estimation block estimates the states for the EOL model,  $\mathbf{x}_{\text{EOL}}(k)$ , based on the data from the previous discharge cycle. In the context of the EOD model,  $\mathbf{x}_{\text{EOL}}(k)$  are the aging parameters and assumed to be constant for a given discharge. The state estimation block estimates states for the EOD model,  $\mathbf{x}_{\text{EOD}}(k)$ , using the latest estimates of the aging parameters. EOD prediction computes the probability distribution of the EOD time,  $k_{\text{EOD}}$ , using the latest state estimate and aging parameter estimates. The aging rate parameters,  $\theta_{\text{EOL}}(k)$  for the EOL model are estimated based on the estimated aging parameters over past discharge cycles, and parameterize how quickly the aging parameters change in time. EOL prediction computes the probability distribution of the EOL time,  $k_{\text{EOD}}$ , using the current estimates of the aging and aging rate parameters.

## VIII. Uncertainty Representation

The reasons to build frameworks capable of accommodating uncertainty are several, and have already been extensively discussed in literature.<sup>16</sup> First, the selection of certain model granularity, together with the choice of the state variables, defines the representation capabilities of the health management system. Un-modeled physical phenomena and states of the system that are ignored by the model contribute to uncertainty in the monitored state variables and model parameters. The state variables are, in most cases, un-observable, and therefore estimators from available sensor data of such hidden states are necessary to characterize the current condition of the system. Tools and sensors utilized to measure the observable quantities are themselves affected by limited accuracy and precision, which may also depend on environmental conditions, which are aleatory in nature. Therefore, it is clear how the comprehensive diagnostic and prognostic framework presented in this paper requires uncertainty quantification methods to establish the confidence over the estimated variables, as well as reduce uncertainty in the prediction.

The work discussed in this section is inspired by the approach for uncertainty quantification of vehicle

health recently proposed in,<sup>17</sup> and it concentrates on representing uncertainty within elements of the powertrain model. Uncertainty quantification for each element of the system is left to future research, where assessment of model performance against experimental evidence will aid the quantification process.

### A. Uncertainty in the battery model

The output voltage represents the quantity of interest, which defines the energy introduced in the powertrain to produce the desired torque. A sampling-based approach is suggested for the battery model, given its nonlinear state-space model presented in Section V.A. The state vector in the first row of Eq. 16 actually contains two independent variables, that is the amount of Li-ions on the positive side of the surface  $q_{s,p}$  and bulk  $q_{b,p}$  of the cell, respectively. Since  $q_{s,n}$ ,  $q_{b,n}$ , and the different voltages  $V'$  are derived quantities, they also become random variables because of their relationship to  $q_{s,p}$  and  $q_{b,p}$ .

The uncertainty affecting the number of Li-ions on the elements of the cell is modeled by perturbations of the state transition equation, using properly-scaled random shocks:

$$\begin{aligned} q_{s,p,k} &= q_{s,p,k-1} + \dot{q}_{s,p,k-1} \Delta t_{k-1} + \sigma_{q_{s,p}} \sqrt{\Delta t_{k-1}} r_1 \quad , \\ q_{b,p,k} &= q_{b,p,k-1} + \dot{q}_{b,p,k-1} \Delta t_{k-1} + \sigma_{q_{b,p}} \sqrt{\Delta t_{k-1}} r_2 \quad . \end{aligned} \quad (24)$$

The perturbations are represented by  $\sigma_{q_{s,p}} r_1$ ,  $\sigma_{q_{b,p}} r_2$ , where  $r_i, i = \{1, 2\}$  are random realizations from a standard normal distribution. They are scaled by  $\sqrt{\Delta t}$  so that the variance of the stochastic processes scales linearly with time. Such a scaling is in agreement with formulations of stochastic differential equations.<sup>18</sup> It should be noticed that the behavior of the stochastic processes in (24) is close to a diffusion process, being the variables unbounded, and more advanced representations could be used to better represent the movements of the ions at the very early stage and end of the battery life.

### B. Uncertainty representation in the ESC model

The ESC circuit model is composed of three fundamental elements, as already presented in Eq. (17). The SPWM signals  $F_i$ ,  $i = \{1, 2, 3\}$ , the switch matrix, and the voltage from the battery. The frequency carrier of the SPWM signals may slowly decrease as time passes by because of MOSFET degradation.<sup>5</sup> This implies a monotonic behavior of the SPWM carrier frequency, and therefore its uncertainty should not be represented by a diffusion process similar to the one utilized in A, but it should reflect its monotonic behavior. Decreasing carrier frequencies could be modeled using a negative, log-Normally distributed rate of change, as in Eq. (25).

$$\begin{aligned} f_k &= f_{k-1} - \left. \frac{df}{dt} \right|_{k-1} \exp \eta \\ \eta &\sim \mathcal{N}(-\sigma_\eta^2/2, \sigma_\eta^2) \end{aligned} \quad (25)$$

The correction of the mean value of  $\eta$ , i.e.,  $-\sigma_\eta^2/2$ , ensures that the stochastic process is centered on its mean value regardless of the selected variance  $\sigma_\eta^2$ , i.e.,

$$\mathbb{E} \left[ \left. \frac{df}{dt} \right|_k \exp \eta \right] = \left. \frac{df}{dt} \right|_k \quad . \quad (26)$$

This degradation is expected to be slow, and its effect likely to be negligible in a single flight.

Switch matrix failures may be easily represented using typical reliability analysis,<sup>19</sup> therefore using time-dependent failure rates  $\lambda(t)$ , mean time between-failures, or similar quantities. When a switch fails, the corresponding switch matrix element in (17) becomes zero, representing the effect of a switch that no longer closes (or opens).

### C. Uncertainty representation in the motor model

Given the consolidated structure of the motor model, widely utilized to describe DC motor dynamics, uncertainty in the model structure is not considered in this preliminary work. Moreover, the uncertainty on

the external loading is not discussed and left to future research. In this work, we assume the motor model parameters could be described by random variables to encapsulate motor parameter uncertainty. Because of their physical meaning, all model parameters  $\theta = [B, J, R_s, L_M]^T$  have to be positive, so  $\theta_i \in \mathbb{R}^+ \forall \theta_i \in \theta$ . Gaussian distributions may not be suitable to describe the uncertainty on those model parameters, since Gaussian distributions are unbounded. This may create problems especially in real-time parameter estimation and updating, Bayesian filtering, etc. where erroneous measures or spurious correlations can lead the estimations outside of the (physical) parameter support space. Weibull, log-Normal and Gamma are examples of distributions suitable for positive-definite model parameters.

## IX. Discussion and Comments

In this work an framework for e-UAS health monitoring is developed integrating an FMECA based Qualitative Bayesian approach with Diagnostics and Prognostics framework. An e-UAS system comprises of several sub-systems and components. Before implementing a tool like Diagnostics and Prognostics on-board an e-UAS vehicle it is very important to identify essential sub-systems components which have a high probability failure rate. This enables the diagnoser tool to identify and isolate systems in case of any failure or degradation. Once the culprit is accurately identified an prognoser is instantiated to estimate remaining useful life and further take decisions based on operational requirements.

Implementing such a framework especially on e-UAS vehicles reduces the computational power requirement on-board where is only systematically identified sub-system and components are monitored instead of the whole set. In addition the framework also incorporates sensor noise, modeling imperfections and estimation errors.

In this work an Qualitative Bayesian approach was discussed. Our next research goal is working towards a combined qualitative and quantitative approach for e-UAV. Work in currently underway to evaluate the developed FEMCA to quantitative failure rates and probabilities to be updated in table and implement in the Bayesian framework.

## References

- <sup>1</sup>Roychoudhury, I., Biswas, G., and Koutsoukos, X., "Distributed diagnosis in uncertain environments using dynamic bayesian networks," *Control & Automation (MED), 2010 18th Mediterranean Conference on*, IEEE, 2010, pp. 1531–1536.
- <sup>2</sup>Hogge, E., Bole, B., Vazquez, S., Kulkarni, C., Strom, T., Hill, B., Smalling, K., and 8, C. Q., "Verification of Prognostic Algorithms to Predict Remaining Flying Time for Electric Unmanned Vehicles," *International Journal of Prognostics and Health Management, ISSN 2153-2648, 2018 021*, 2018.
- <sup>3</sup>Kulkarni, C. S., Celaya, J. R., Biswas, G., and Goebel, K., "Towards A Model-Based Prognostics Methodology for Electrolytic Capacitors: A Case Study Based on Electrical Overstress Accelerated Aging," *International Journal of Prognostics and Health Management*, Vol. 5, No. 1, 2012, pp. 16.
- <sup>4</sup>Daigle, M., Sankararaman, S., and Kulkarni, C., "Stochastic Prediction of Remaining Driving Time and Distance for a Planetary Rover," *2015 IEEE Aerospace Conference*, March 2015.
- <sup>5</sup>Gorospe, G., Kulkarni, C., and Hogge, E., "A Study of the Degradation of Electronic Speed Controllers for Brushless DC Motors," *Asia Pacific Conference of the Prognostics and Health Management Society*, 2017.
- <sup>6</sup>Gorospe, G. E. and Kulkarni, C. S., "A novel UAV electric propulsion testbed for diagnostics and prognostics," *IEEE AUTOTESTCON*, 2017.
- <sup>7</sup>HUMPHREYS, M. and JACOBS, A., "Mixing Methods: A Bayesian Approach," *American Political Science Review*, 2015.
- <sup>8</sup>Medow, M. and Lucey, C., "A qualitative approach to Bayes' theorem," *BMJ Evidence-Based Medicine*, 2011.
- <sup>9</sup>Kulkarni, C. S., Roychoudhury, I., and Gorospe, G. E., "Distributed Diagnosis of Electric Aircraft Powertrain," *PROCEEDINGS OF THE EUROPEAN CONFERENCE OF THE PHM SOCIETY*, Vol. 4, PHM Society, 2018.
- <sup>10</sup>Rahn, C. D. and Wang, C.-Y., *Battery Systems Engineering*, Wiley, 2013.
- <sup>11</sup>Daigle, M. and Kulkarni, C., "Electrochemistry-based Battery Modeling for Prognostics," *Annual Conference of the Prognostics and Health Management Society 2013*, Oct. 2013, pp. 249–261.
- <sup>12</sup>Karthikeyan, D. K., Sikha, G., and White, R. E., "Thermodynamic model development for lithium intercalation electrodes," *Journal of Power Sources*, Vol. 185, No. 2, 2008, pp. 1398–1407.
- <sup>13</sup>Roychoudhury, I., Biswas, G., and Koutsoukos, X., "Designing distributed diagnosers for complex continuous systems," *IEEE Transactions on Automation Science and Engineering*, Vol. 6, No. 2, 2009, pp. 277–290.
- <sup>14</sup>Daigle, M. and Goebel, K., "Model-based Prognostics with Concurrent Damage Progression Processes," *IEEE Transactions on Systems, Man, and Cybernetics: Systems*, Vol. 43, No. 4, May 2013, pp. 535–546.
- <sup>15</sup>Daigle, M. and Sankararaman, S., "Advanced Methods for Determining Prediction Uncertainty in Model-Based Prognostics with Application to Planetary Rovers," *Annual Conference of the Prognostics and Health Management Society 2013*, October 2013, pp. 262–274.

<sup>16</sup>Sankararaman, S., “Significance, interpretation, and quantification of uncertainty in prognostics and remaining useful life prediction,” *Mechanical Systems and Signal Processing*, Vol. 52, 2015, pp. 228–247.

<sup>17</sup>Corbetta, M. and Kulkarni, C. S., “An Approach for Uncertainty Quantification and Management of Unmanned Aerial Vehicle Health,” *Proceedings of the Annual Conference of the Prognostics and Health Management Society 2019*, Vol. in press, 2019.

<sup>18</sup>Lawler, G. F., “Stochastic Calculus: An Introduction with Applications,” *American Mathematical Society*, 2010.

<sup>19</sup>Ginart, A., Brown, D., Kalgren, P., and Roemer, M., “Online Ringing Characterization as a Diagnostic Technique for IGBTs in Power Drives IGBTs in Power Drives,” *IEEE Transactions on Instrumentation and Measurement*, Vol. 58, 2009.